Journal of Geological Resource and Engineering 6 (2018) 194-209
doi:10.17265/2328-2193/2018.05.002

GPR Survey for Fir (*Abies alba*) and Spruce (*Picea abies*) Root Systems in Different Locations in the Western Carpathians Mts. (Poland)

Bożena Potępa[1], Adam Szynkiewicz[2] and Magdalena Udyrysz-Kraweć[3]

1. Siedliska Naturalne, 57-200 Ząbkowice Śląskie, Zwrócona 28, Poland

2. Kart-Geo 51-649 Wrocław, Bacciarellego 39/1, Poland

3. Sumo Services, Upton Upon Severn, Worcestershire, England

Abstract: The aim of the GPR research was a non-invasive inspection of the root systems arrangement of selected trees (fir *Abies alba* and spruce *Picea abies*), in the Silesian Beskids Landscaped Park and Żywiec Beskids Landscaped Park (Carpathian Mountains, Poland). Field research has been done using RAMAC/GPR with 800 MHz shielded antennas. The survey was conducted by linear profiling to a depth of 2 m. The survey was carried out around the designated trees in 6 meters × 6 meters grids. Base points for X (S-N) and Y (W-E) axis were set in corners of each grid. Parallel GPR traverses were conducted within each study area, at intervals of 0.20 m. The maps of the research areas show existing trees and stumps within the GPR sections, with ±0.1 m error. GPR data analysis was carried out in 2D and 3D systems. Major findings from the GPR survey concluded that the firs (*Abies alba*), have a "vertical" root system type (with the roots dominant at depths of 0.2-0.8 meters), concentrically away from the tree trunk at a distance of about 1 m to about 2 m, and the spruces (*Picea abies*), have a "cloud" root system type (at a depth of 10-100 cm), with a few clear, thicker roots extending from the trunk.

Key words: GPR, root systems fir and spruce, Carpathian Mts., Poland.

1. Introduction

In the mountain landscape parks of the Silesian Beskids and the Beskid Żywiecki Western Carpathians (Fig. 1), the predominant forest habitats are: fresh mountain forest and mixed fresh mountain forest. The age of the forest is about 40-60 years. In many places the trees are unhealthy, this is due to the inadequate selection of trees for habitat conditions at planting sites. Therefore, it is necessary to replace the stands, especially for fir and spruce. Forests have been subject to detailed research in the indicated areas.

One of the projects' concerns was to obtain detailed studies of the condition of selected forest habitats. This project is financed by the Regional Fund for Environmental Protection in Katowice and run jointly with the Regional Directorate of State Forests in Katowice. As part of a scientific and research study on the analysis of soil conditions of fir in the forests of the Beskid Śląski and Żywiecki (538/BR/16), research on the root systems of: fir and spruce trees using the GPR method was carried out at selected positions.

Ground-penetrating radar (GPR) is a safe and valuable method for the non-destructive testing of ground structures [1-6]. There is a lot of work in the scientific literature regarding the effective use of GPR for the assessment of root systems of trees [7-29].

1.1 Research Stands

In the Landscape Parks of the Silesian Beskids and the Żywiecki Beskids (Western Carpathians Mts.), five stands have been designated for the examination of root systems of selected trees (Fig. 2). These research sites are located in forested mountainous areas.

Corresponding author: Adam Szynkiewicz, PhD, research fields: GPR method, geology of Cenozoic, geology of karst.

Fig. 1 Western Carpathians Mts. The area (red star) of researching tree roots using the GPR method [49°30′17″ N; 19°01′00″ E].

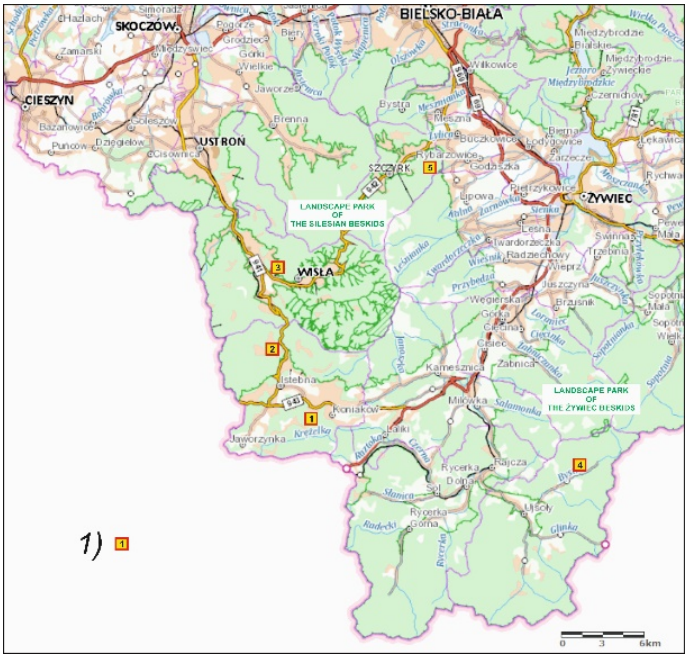

Fig. 2 Western Carpathians Mts. Beskid Śląski and Beskid Żywiecki. Forests are marked in green.

1.1.1 Sites of GPR Research

(1) Research site 1 (Wisła Forest District, No. 107A Zapowiedź)

GPR tests were carried out on a surface with dimensions: 6 m × 6 m, around the tree No. 1: fir (Fig. 3). The area is located at an altitude of about 700 m above sea level and is located on a slope inclined north-west. Mountain soils developed here on sandstone and shale (age of rocks: Upper Cretaceous, senon). Cracked Upper Cretaceous rocks are inclined towards the south [30].

(2) Research site 2 (Wisła Forest District, No. 15A Olza)

GPR tests were carried out on a surface with dimensions: 6 m × 6 m, around the tree No. 2: spruce (Fig. 4). The area is located at an altitude of about 540 m above sea level, and is located on a slope inclined west. Mountain soils developed here on shale rocks (age of rocks: Upper Cretaceous). Cracked Upper Cretaceous rocks are inclined south-west [30].

Fig. 3 Site 1: fir.

Fig. 4 Site 2: spruce.

(3) Research site 3 (Wisła Forest District, No. 46B Kubalonka)

GPR tests were carried out on a surface with dimensions: 6 m × 6 m, around the tree No. 3: spruce (Fig. 5). The area is located at an altitude of about 800 m above sea level and is located on a slope inclined south-west. Soils developed here on sandstones (age of rocks: Upper Cretaceous). Cracked Upper Cretaceous rocks are inclined towards the south [30].

(4) Research site 4 (Ujsoły Forest District, No. 21D Zlatna)

GPR tests were carried out on a surface with dimensions: 6 m × 6 m, around the tree No. 4: fir (Fig. 6). The area is located at an altitude of about 1,000 m above sea level and is located on a slope inclined south. Soils developed here on sandstones (age of rocks: Paleogene). Cracked Paleogene rocks are inclined towards the south [31].

(5) Research site 5 (Bielsko-Biała Forest District, No. 134 Skalite, shown in Fig. 7)

GPR tests were carried out on a surface with dimensions: 6 m × 6 m, around the tree No. 5: fir (Fig. 7). The area is located at an altitude of about 600 m above sea level and is located on a slope inclined south. Soil is developed here on shales intercalated with sandstone (age of rocks: Upper Cretaceous, cognac-mastricht). The Upper Cretaceous rocks are inclined south-west [32].

1.2 Ground Water

The sites designated for GPR research are located in areas of low mountains (500-1,000 m above sea level). There are soils developed on the debris and weathered rocks: sandstones and shales. For mountainous areas, zones with diverse groundwater conditions are distinguished [33]. In reference to the topographical and geological situation of the research stands, it can be assumed that there are also groundwater zones described below, affecting soil humidity:

Zone I: a weathering cover with variable thickness,

Fig. 5 Site 3: spruce.

Fig. 6 Site 4: fir.

Fig. 7 Site 5: fir.

high water capacity and low water conductivity: thickness of the wet zone m = 1-10 m; effective porosity n = 0.24; filtration coefficient k = 0.1 m/day; gravitational drainage u = 0.12.

Zone II: weathered and strongly cracked rocks, variable thickness, medium water capacity and low water conductivity: thickness of the wet zone m = 10-50 m; effective porosity n = 0.01-0.05; filtration coefficient k = 1 m/day; gravitational drainage u = 0.008-0.03.

Zone III: zone of deep circulatory pathways, which includes cracks accompanying fault zones, has the lowest capacity and hydraulic conductivity: thickness of the wet zone m = 100-500 m; effective porosity n = 0.0001-0.01; filtration coefficient k = 0.001-0.1 m/day; gravitational drainage u = 0.0008-0.001.

2. Methodology of GPR Research

2.1 Methodology of Field Research

Field radar surveys (GPR) were carried out with a portable RAMAC/GPR, powered by 12 V batteries.

Shielded antennas with a central frequency of 800 MHz are used for profiling. They were moved along the ground surface. Distances were measured with a measuring wheel (Fig. 8). The tests were carried out by linear profiling to a depth of 2 m.

In the above-mentioned sites, free-standing trees were designated (Figs. 3-7), whose root systems were to be tested with the GPR method: No. 1 (fir), No. 2 (spruce), No. 3 (spruce), No. 4 (fir), No. 5 (fir).

Around the examined trees, control points were designated: A, B (X axis) and then at points 6 m away from them designated points: A1 and B1 were established. In this way, research squares with dimensions of 6 × 6 m were created. Measuring tapes were arranged between points A and B and points A1 and B1 (Fig. 9). For all research areas, the Y axis has always had the direction S-N. The Y axis has always been on the western side of the studied tree. Within each of the GPR survey area, cross-sectional lines were run in the same direction (from the south towards the

Fig. 8 Ground penetrating radar (RAMAC/GPR) with an 800 MHz antenna (GPR field measurement method).

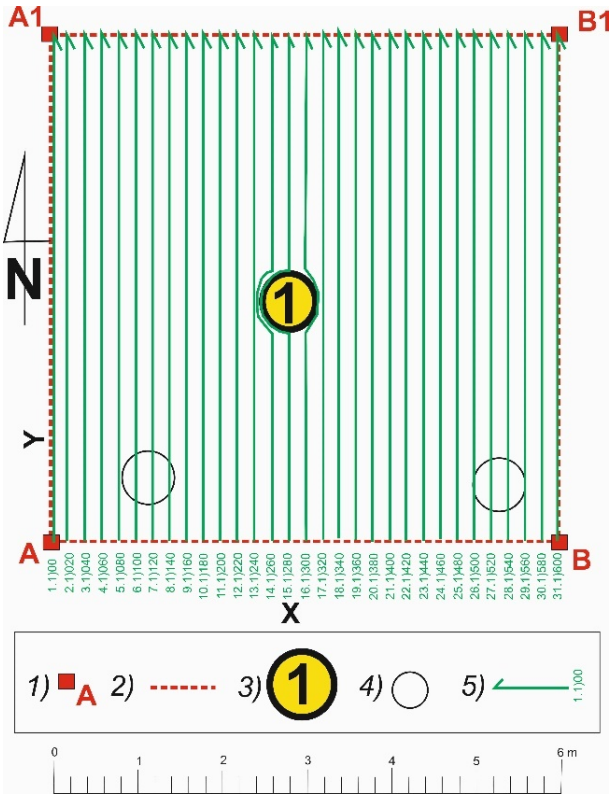

Fig. 9 An example of a sketch of the location of GPR sections. 1) Control points; 2) baselines, measuring tapes; 3) the location of the tree whose root system is examined; 4) carp, stumps; 5) GPR section.

north), parallel to each other, at intervals of 0.20 m. Each cross-sectional line was marked with a number and distance from the point (0, 0) (on the X and Y axes). On the sketches of research areas, georadar cross-section lines (GPR) were marked with green arrows, with an accuracy of ±0.1 m (Fig. 9). The stumps of felled trees, or other trees existing in the area of the study were also marked on these sketches.

2.2 Methodology for Interpreting GPR Data

A trial analysis of GPR data in the 3D system was done by Magdalena Udyrysz (SUMO SERVICES, England). After entering data into the 3D program and subjecting it to filtration, horizontal time slices, vertical time slices and block images of the GPR anomalies were obtained.

An example of all GPR anomalies seen from above is shown in Fig. 10. Brown colors show root systems (soft elements). With a circle, dash broken in indigo, the forecasted range of the root system of the examined tree was marked.

Horizontal time slices from selected depths are shown for each site (Figs. 11, 13, 15, 16, 18). In these figures, the blue colors show hard places such as rock or weakly cracked rock. However, the colors: red, orange and yellow—are anomalies showing "soft" places (e.g. roots). The dotted line, in the indigo color, shows the predicted range of the root system of the examined tree at a given depth.

From numerous vertical time-slices few selected cross-sections illustrating the vertical ranges of the root systems studied (Figs. 12, 14, 17, 19) have been shown. In these figures, the blue colors show hard places such as rock or weakly cracked rock. However, the colors: red, orange, yellow—are anomalies showing "soft" places (e.g. roots). The dotted line, in indigo, shows the predicted range of the root system of the examined tree.

The example of station No. 5 (Fig. 20) also shows the block image of all anomalies, seen from the side. The dotted line in indigo shows the range of the root system of the examined tree.

3. Results

3.1 Site 1 (Fir)

Block image.

On a top view of all anomalies (Fig. 10), echoes converging concentrically from the main root system

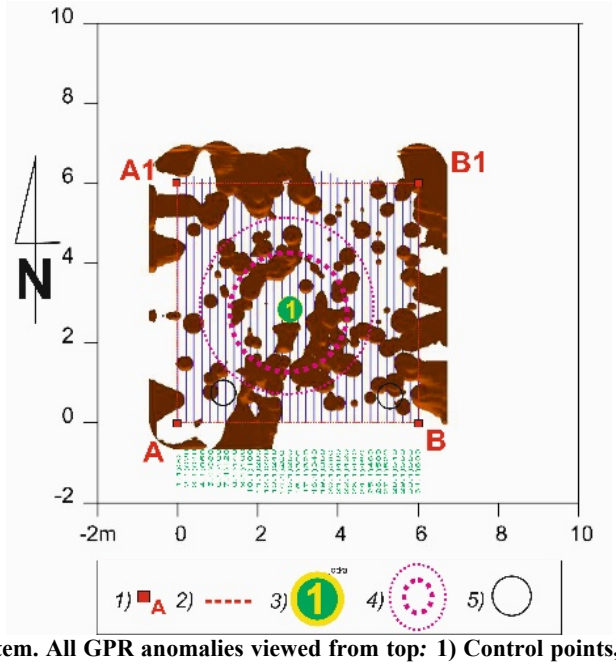

Fig. 10 Site 1. Fir tree root system. All GPR anomalies viewed from top: 1) Control points, 2) baselines, 3) location of trees whose root system is examined, 4) range of the root system of the examined tree, 5) capro, stump.

can be seen. The image indicates the "vertical" arrangement of the main root system. Intermediate indigo lines indicate the possible range of the main root system of the examined tree 1 (fir).

Horizontal time slices, for selected depths (0.32-0.38 m; 0.38-0.43 m; 0.49-0.54 m; 0.70-0.76 m), show a general view of the root system (Fig. 11). The main tree root system is arranged concentrically (circle, dashed line in indigo), up to a distance of about 1 meter from the trunk of the tree (fir). Strong echoes from the main root system occur at depths: from 0.2 to 0.76 meters.

Analysis of vertical time slices confirms the "finger" nature of the main root system. The selected image of the vertical time slices is shown in Fig. 12, in which the possible root range of the examined tree is marked with a dotted line in the indigo color.

3.2 Site 2 (Spruce)

On horizontal time slices, from selected depths (Fig. 13), a general picture of the distribution of GPR anomalies seen from above is shown. Roots (soft elements) are, marked with colors red, yellow and orange. Around the tree No. 2, the root system forms a dense network ("cloud" of small roots), which is marked by a circle of dashed line in indigo. The largest accumulation of roots is in depths: 0.15-1.00 m.

The analysis of vertical time cuts confirms the above observations (Fig. 14), and the dashed line indicates the

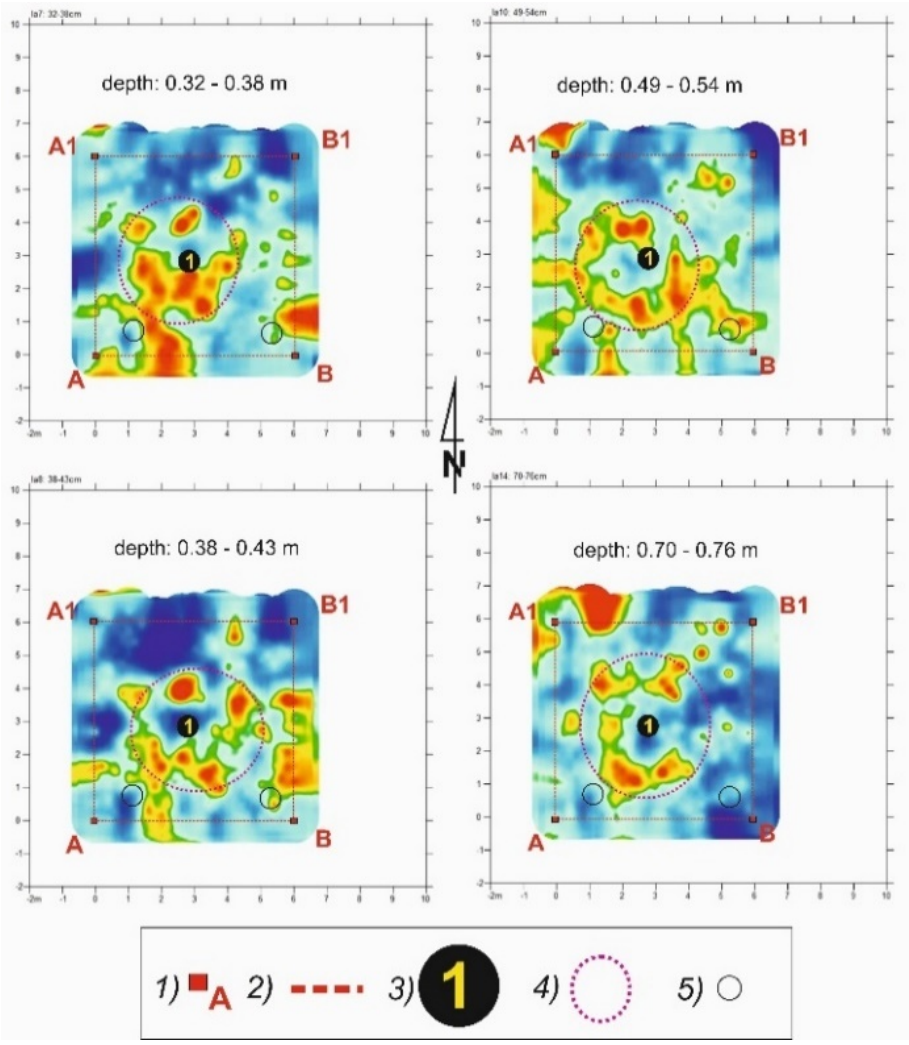

Fig. 11 Site 1. Fir tree root system. GPR anomalies viewed from top on selected horizontal time slices from depth of: 0.32-0.76 m (as explained in Fig. 10).

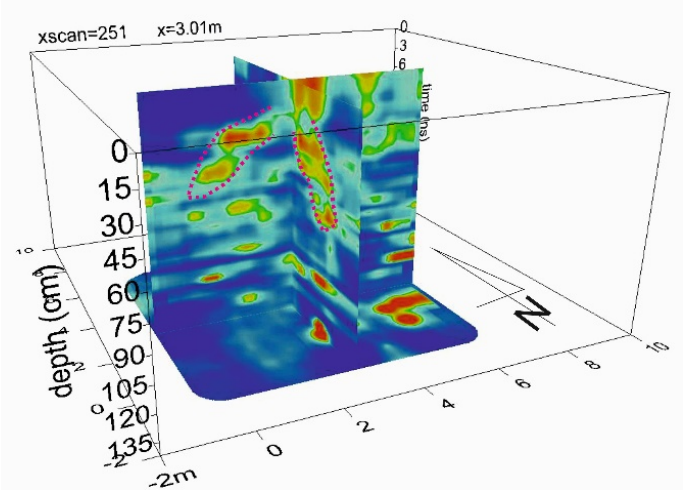

Fig. 12 Site 1. GPR anomalies—on selected vertical time slices. Fir tree root system showing a dotted indigo line.

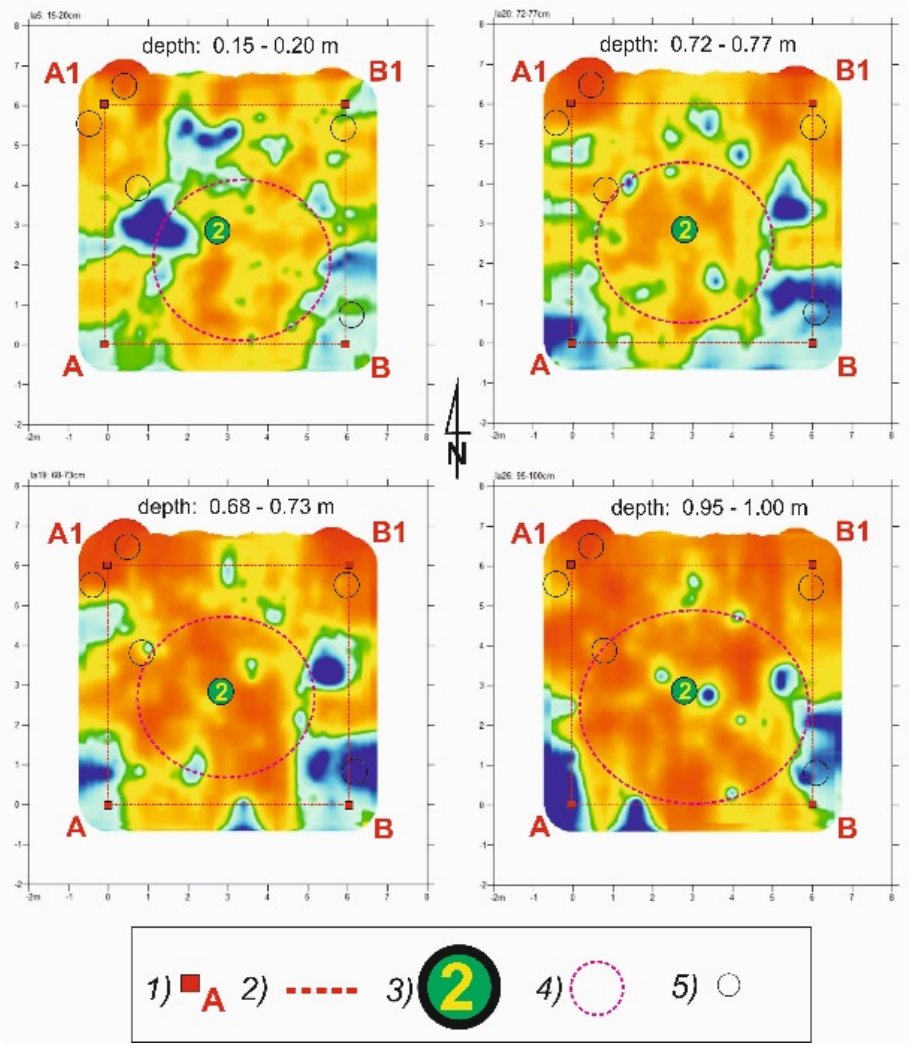

Fig. 13 Site 1. Spruce tree root system. GPR anomalies viewed from top on selected horizontal time slices from depth of: 0.15-1.00 m (as explained in Fig. 10).

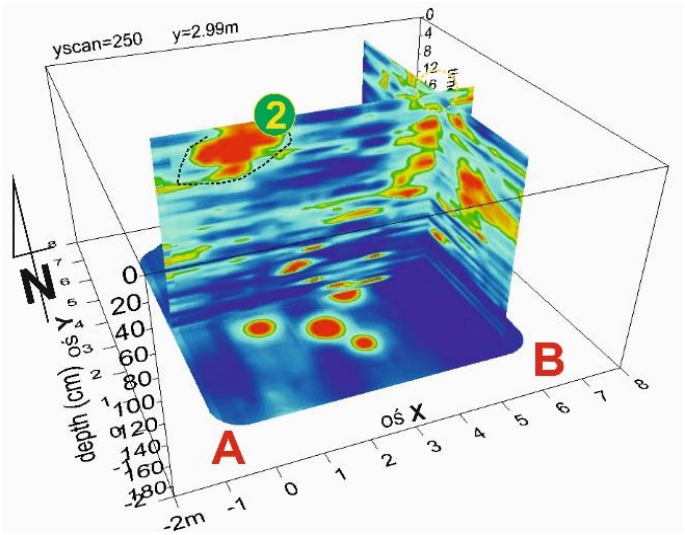

Fig. 14 Site 2. GPR anomalies—on selected vertical time cuts. The spruce tree root system shows a dotted black line.

possible depth of the root system of the examined tree 2 (spruce).

3.3 Site 3 (Spruce)

On horizontal time slices, from selected depths (Fig. 15), a general picture of the distribution of GPR anomalies seen from above is shown. Roots (soft elements) are, marked with colors red, yellow and orange. Around the tree No. 3, the root system forms a dense network ("cloud" of small roots), which is marked by a circle of dashed line in indigo. The largest accumulation of roots is in depths: 0.54-1.02 m.

3.4 Site 4 (Fir)

Horizontal time slices, for selected depths (0.35-0.41 m; 0.48-0.54 m; 0.83-0.89 m; 0.92-0.98 m), show a general view of the root system (Fig. 16). The main root system of the tree is laid "finger-like" (dashed line in indigo), up to a distance of about 1 meter from the trunk of the tree (fir). Strong echoes from the main root system occur at depths from 0.3 to 1.0 meters. The observation that this fir has "finger-like" character of the main root system is confirmed by the analysis of vertical time slices. Selected images of vertical time cuts show the possible range of the root system of the examined tree (Fig. 17). Tree 4 (fir) has vertically ("finger-like") developed its main root system, at which the "cloud" developed a root system of small roots.

3.5 Site 5 (Fir)

Horizontal time slices, for selected depths: 0.32-0.96 m, show the overall picture of the root system (Fig. 18). The main root system of the tree is laid "finger-like" (dashed line in indigo), up to a distance of about 1 meter from the trunk of the tree (fir). Strong echoes from the main root system occur at depths from 0.3 to 1.0 meters. This observation is confirmed by the analysis of vertical time slices, confirming the "finger-like" character of the main root system. The selected image of the vertical time slices shows the possible vertical range of the root system of the examined tree (Fig. 19). Tree 4 (fir) has vertically ("finger-like"), developed main root system, at which the "cloud" developed a root system of small roots. A block view of the entire root system seen from the east confirm that this fir has a "finger-like" root system (Fig. 20).

3.6 Excavation

In the vicinity of trees whose root systems were subjected to GPR testing, inspection pits (excavation) were dug to a depth of about 1.0 m. Data from these exposures are consistent with GPR surveys. Firs have

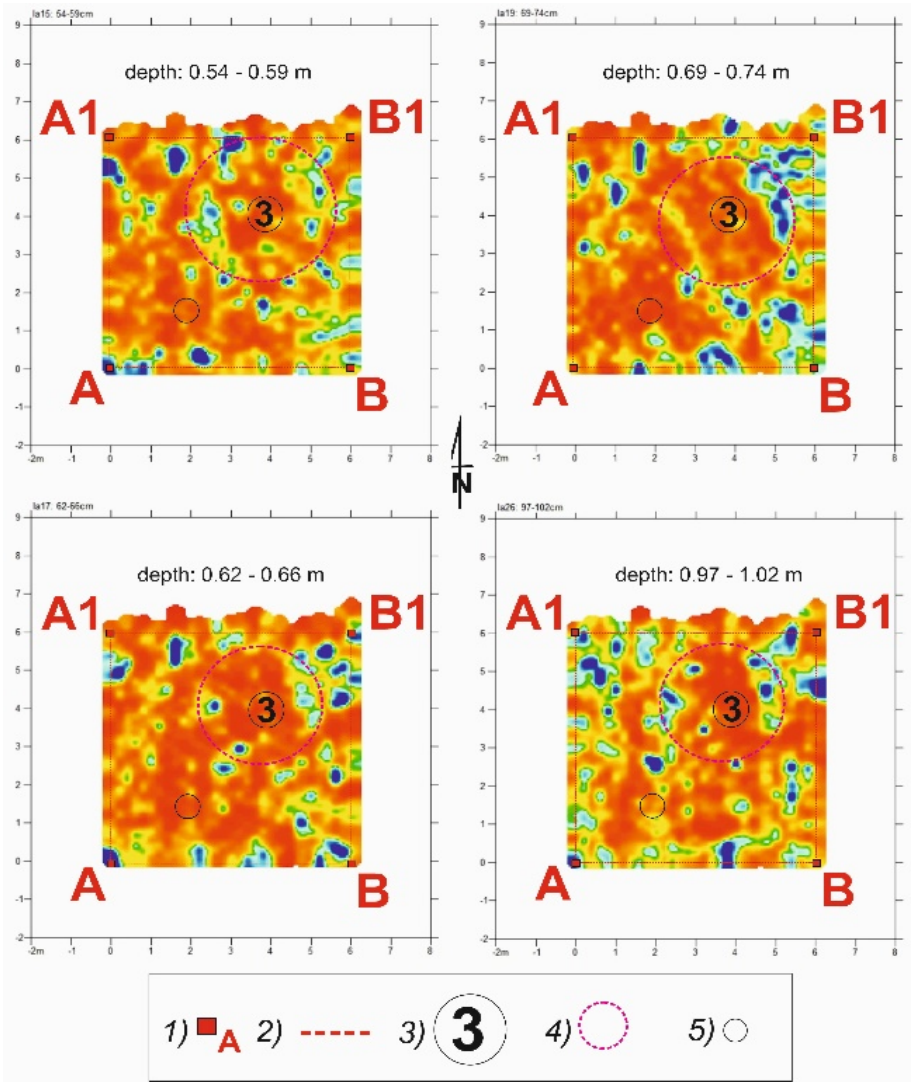

Fig. 15 Site 3. Spruce tree root system. GPR anomalies—view from top on selected horizontal time slices from depth of: 0.54-1.02 m (as explained in Fig. 10).

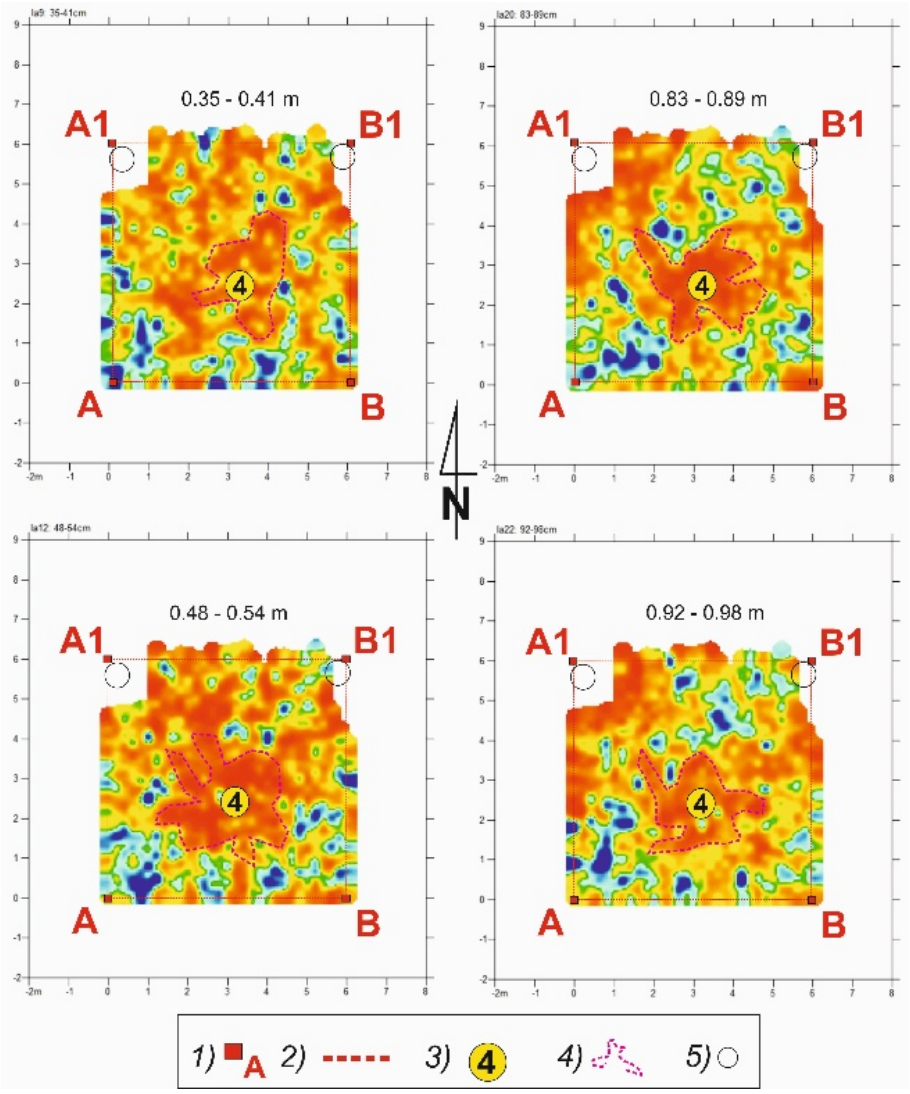

Fig. 16 Site 4. Fir tree root system. GPR anomalies—view from top on selected horizontal time slices from depth of: 0.32-0.76 m (as explained in Fig. 10).

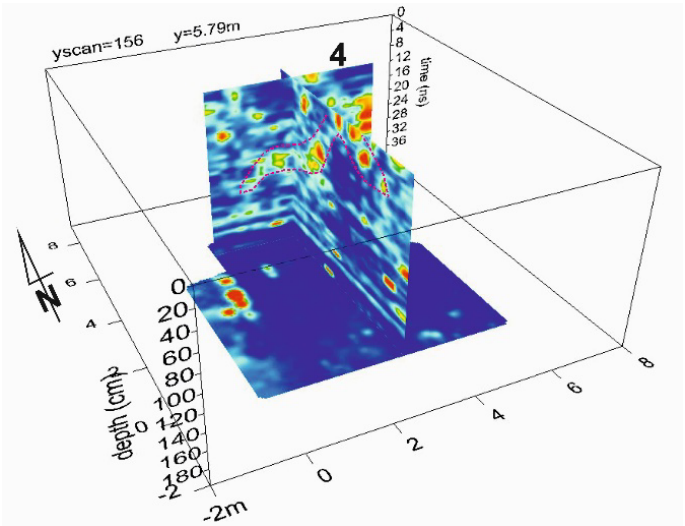

Fig. 17 Site 4. GPR anomalies—on selected vertical time slices. Fir tree root system showing a dotted indigo line.

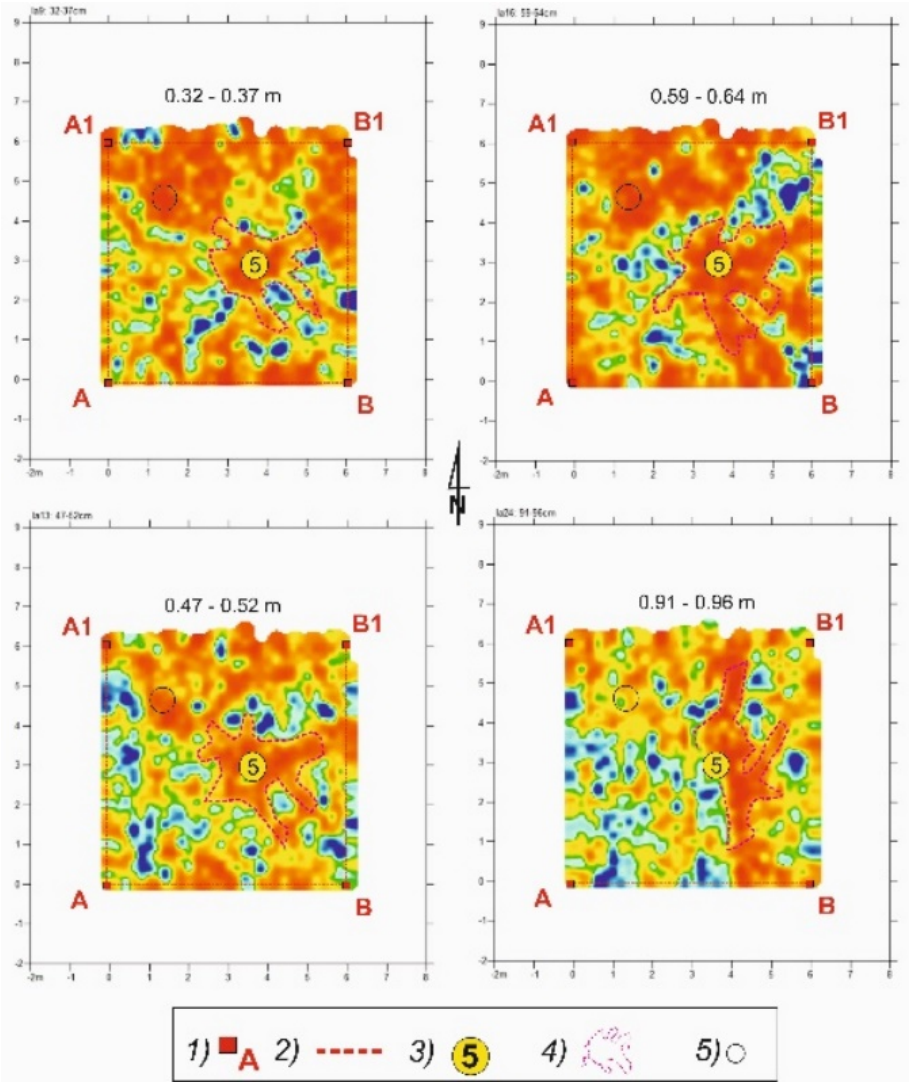

Fig. 18 Site 5. Fir tree root system. GPR anomalies—view from top on selected horizontal time slices from depth of: 0.32-0.96 m (as explained in Fig. 10).

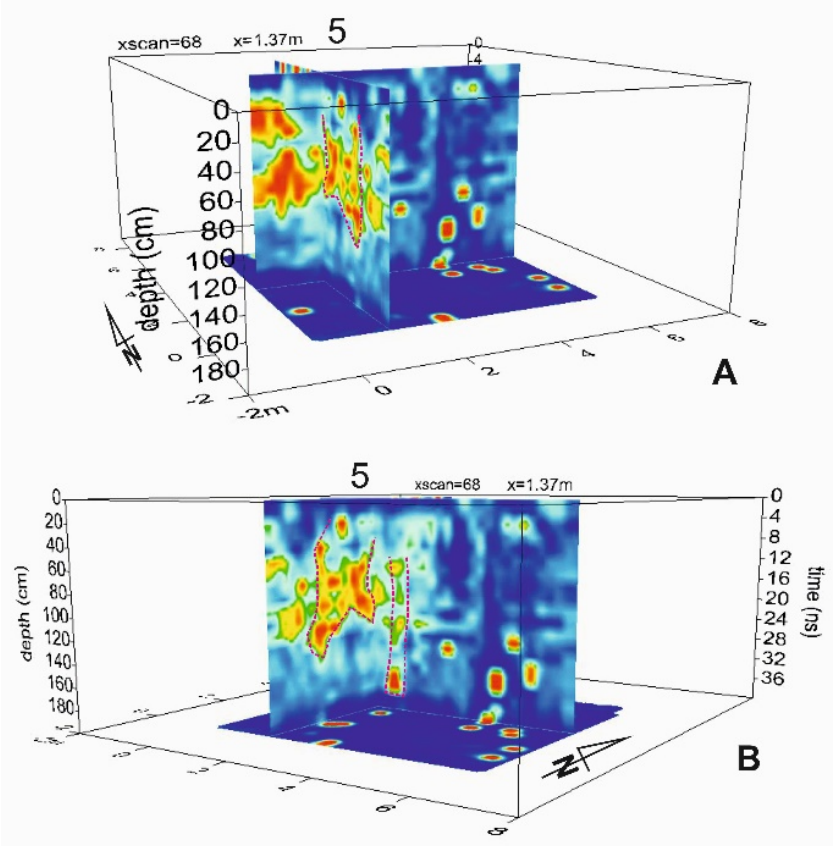

Fig. 19 Site 5. GPR anomalies—on selected vertical time slices. Fir tree root system showing a dotted indigo line.

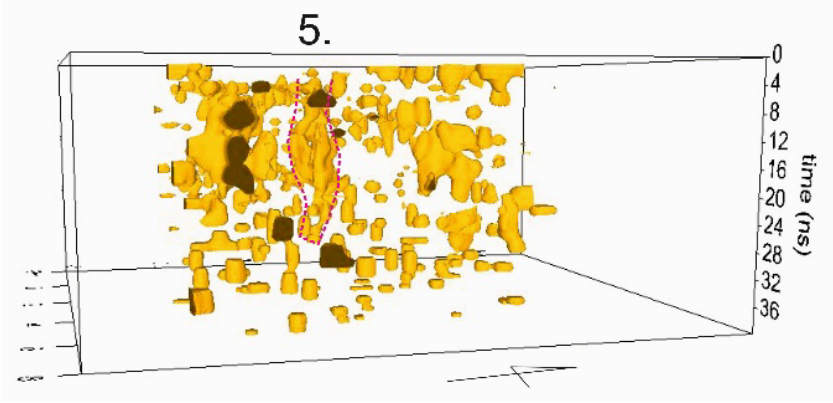

Fig. 20 Site 5. GPR anomalies—block image of fir tree root system (dotted indigo line) seen from the east.

Fig. 21 Site 1. Fir tree root system in pit.

Fig. 22 Site 2. Spruce tree root system in pit.

Fig. 23 The root system of fallen spruce tree (oval in yellow).

"finger-like" developed systems of main roots that penetrate deeply into the rock crevices and a small number of fine roots (Fig. 21). Spruce trees have many small roots ("cloud"). Their dense systems reach a shallow depth (Fig. 22). The "cloud" of a spruce root system is clearly visible when such a tree is knocked down as a result of strong wind (Fig. 23).

4. Conclusions

The following conclusions emerge from the analysis of georadar data (GPR):

(1) GPR studies of the root systems of fir and spruce trees were carried out on selected forest research areas, located at altitudes of 500-1,000 m above sea level, in the Western Carpathians Mts.

(2) Within the studied areas, mountain soils occur, on debris from strongly fractured rocks.

(3) Soil of sites: 1, 3, 4, 5 are on sandstone, while the soil of site 2 is on shale.

(4) Firs have "finger-like" developed main root systems, pushing "vertically" into rock crevices up to 2.0 m depth and a few small roots.

(5) Spruce have "cloud" developed root systems (numerous, dense, small, thin roots), reaching to a depth of about 1 meter.

(6) The GPR method allows for very detailed horizontal and vertical depiction of tree root systems.

Acknowledgments

Work was done jointly with Regional Directorate of State Forests in Katowice, financed by Regional Fund for Environmental Protection (WFOŚ) in Poland.

The authors thank Prof. Lara Pajewski from the Sapienza University of Rome (Italy) for the inspiration of GPR research.

This work is a contribution to COST (European Co-operation in Science and Technology) Action TU1208 "Civil Engineering Applications of Ground Penetrating Radar" (www.cost.eu, www.GPRadar.eu). The authors thank COST for funding and supporting the Action TU1208.

References

[1] Ulriksen, P. F. 1982. "Application of Impulse Radar to Civil Engineering." Doctoral thesis, Lund University of Technology, p. 179.

[2] Daniels, D. J. ed. 2004. *Ground-penatrating Radar*. 2nd ed. IEE Radar, Sonar and Navigation series 15:0-726. The Institution of Electrical Engineers, London. HERTS. MPG Books Ltd. Bodmin Cornwall. UK. ISBN 0 86341 360 9.

[3] Conyers, L. B. 2004. *Ground-Penetrating Radar for Archaeology*. AltaMira Press, p. 203. ISBN 0-7591-0772-6 (0773-4).

[4] Karczewski, J. 2007. *Zarys Metody Georadarowej*. Wydawnictwa AGH (KU 0227), Kraków, p. 246. ISBN 978-83-7464-087-1.

[5] Benedetto, A., Pajewski, L., eds. 2015. "Civil Engineering Applications of Ground Penetrating Radar." In *Springer Transactions in Civil and Environmental Engineering*. Publishing House: Springer International; Book Series April 2015, p. 371.

[6] Wai-Lok Lai, W., Dérobert, X., and Annan, P. 2018. "A Review of Ground Penetrating Radar Application in Civil Engineering: A 30-Year Journey from Locating and Testing to Imaging and Diagnosis." *NDT & E International* 96: 58-78.

[7] Alani Amir, M., Ciampoli, L. B., Tosti, F., Brancadoro, M. G., Pirrone, D., and Benedetto, A. 2017. *Health Monitoring of an Ancient Tree Using Ground Penetrating Radar—Investigation of the Tree Root System and Soil Interaction*. Poster, EGU2017-17210, X4.211. Vienna.

[8] Barton, C. V., and Montagu, K. D. 2004. "Detection of Tree Roots and Determination of Root Diameters by Ground Penetrating Radar under Optimal Conditions." *Tree Physiol*. 24 (12): 1323–31.

[9] Bassuk, N., Grabosky, J., Mucciardi, A., and Raffel, G. 2004. "Ground-Penetrating Radar Accurately Locates Tree Roots in Two Soil Media under Pavement." *Arboric Urban For*. 37 (4): 160.

[10] Borden, K. A., Isaac, M. E., Thevathasan, N. V., Gordon, A. M., and Thomas, S. C. 2014. "Estimating Coarse Root Biomass with Ground Penetrating Radar in a Tree-Based Intercropping System." *Agroforestry Systems* 88 (4): 657-69.

[11] Butnor, J. R., Doolittle, J., Kress, L., Cohen, S., and Johnsen, K. H. 2001. "Use of Ground-Penetrating Radar to Study Tree Roots in the Southeastern United States." *Tree Physiol*. 21 (17): 1269–78.

[12] Butnor, J. R., Doolittle, J., Johnsen, K. H., Samuelson, L., Stokes, T., and Kress, L. 2003. "Utility of Ground-Penetrating Radar as a Root Biomass Survey Tool in Forest Systems." *Soil Sci Soc Am J*. 67 (5): 1607–15.

[13] Butnor, J., Pruyn, M., Shaw, D., Harmon, M., Mucciardi, A., and Ryan, M. 2009. "Detecting Defects in Conifers with Ground Penetrating Radar: Applications and Challenges." *For Pathol.* 39 (5): 309–22.

[14] Butnor, J. R., Barton, C., Day, F. P., Johnson, K. H., Mucciardi, A. N., Schroeder, R., and Stover, D. B. 2011. "Using Ground Penetrating to Detect Tree Roots and Estimate Biomass." In *Measuring Roots: An Updated Approach*, edited by Mancuso S. New York: Springer, pp. 213–46.

[15] Cox, K., Scherm, H., and Serman, N. 2005. "Ground-Penetrating Radar to Detect and Quantify Residual Root Fragments Following Peach Orchard Clearing." *Hort Technology*. 15 (3): 600–7.

[16] Cui, X., Chen, J., Shen, J., Cao, X., Chen, X., and Zhu, X. 2011. "Modeling Tree Root Diameter and Biomass by Ground-Penetrating Radar." *Sci. China Earth Sci.* 54 (5): 711–9.

[17] Delgado, A., Hays, D. B., Selvaraj, M., Ceballos, H., Calle, F., Nevo, A., Goodmand, D., Bruton, R., and Bobreva, I. 2016. Estimation of Below Ground Biomass in Cassava by Ground Penetrating Radar. COST-TU1208, poster v3. gpradar.eu/onewebmedia/Delgado_2016_COST-TU1208_poster_v3.pdf.

[18] Delgado, A., Hays, D. B., Bruton, R. K., Ceballos, H., Novo, A., Boi, E., and Gomez Selvaraj, M. 2017. "Ground Penetrating Radar: A Case Study for Estimating Root Bulking Rate in Cassava (*Manihot esculenta* Crantz)." *Plant Methods* 13: 65. https://doi.org/10.1186/s13007-017-0216-0.

[19] Giża-Potęp, B., Szynkiewicz, A., and Udyrysz, M. 2017. "GPR Survey for Fir (*Abies alba*) and Spruce (*Picea abies*) Root Systems in Different Location in Western Carpathians Mts. (Poland)." EGU GA 2017 (Austria Center Vienna,Vienna, Austria, April 23-28, 2017). Poster: EGU2017-19144, X4.209. Session GI3.1 "Civil Engineering Applications of Ground Penetrating Radar" organized by COST Action TU1208. http://www.egu2017.eu/.

[20] Guo, L., Chen, J., Cui, X., Fan, B., and Lin, H. 2013. "Application of Ground Penetrating Radar for Coarse Root Detection and Quantification: A Review." *Plant Soil* 362 (1–2): 1–23.

[21] Hruska, J., Čermák, J., and Šustek, S. 1999. "Mapping Tree Root Systems with Ground-Penetrating Radar." *Tree Physiol.* 19 (2): 125–30.

[22] Mihai, A., and Gerea, A. 2017. *The Use of Ground Penetrating Radar to Detect Tree Roots in an Urban Setting*. Poster, EGU2017-6867, X4.210. Vienna.

[23] Mancuso, S. 2011. *Measuring Roots: An Updated Approach*. Springer.

[24] Raz, Y. N., Koteen, L., and Baldocchi, D. D. 2013. "Coarse Root Distribution of a Semi-Arid Oak Savanna

Estimated with Ground Penetrating Radar." *J. Geophys. Res. Biogeosci.* 118 (1): 135–47.

[25] Stover, D. B., Day, F. P., Butnor, J. R., and Drake, B. G. 2007. "Effect of Elevated CO_2 on Coarse-Root Biomasses in Florida Scrub Detected by Ground-Penetrating Radar." *Ecology* 88 (5): 1328-34.

[26] Wu, Y., Guo, L., Li, W., Cui, X., and Chen, J. 2014. "Comment on Root Orientation Can Affect Detection Accuracy of Ground-Penetrating Radar." *Plant Soil* 380 (1–2): 441–4.

[27] Wu, Y., Guo, L., Cui, X., Chen, J., Cao, X., and Lin, H. 2014. "Ground-Penetrating Radar-Based Automatic Reconstruction of Three-Dimensional Coarse Root System Architecture." *Plant Soil* 383 (1–2): 155–72.

[28] Yan, H., Dong, X., Feng, G., Zhang, S., and Mucciardi, A. 2013. "Coarse Root Spatial Distribution Determined Using a Ground-Penetrating Radar Technique in a Subtropical Evergreen Broad-Leaved Forest, China." *Sci. China Life Sci.* 56 (11): 1038–46.

[29] Yokota, Y., Matsumoto, M., Gaber, A., Grasmueck, M., and Sato, M. 2011. "Estimation of Biomass of Tree Roots by GPR with High Accuracy Positioning System." In *Proceedings of the 2011 IEEE International Geoscience and Remote Sensing Symposium (IGARSS)*, pp. 190-3.

[30] Burtan, J. 1972. "Detailed Geological Map of Poland 1:50 000, Sheet Wisła." Szczegółowa Mapa Geologiczna Polski 1: 50 000, ark. Wisła (1028). Instytut Geologiczny, Warszawa. (in Polish)

[31] Burtan, J., Sokołowski, S., Sikora, W., and Żytko, K. 1956. "Detailed Geological Map of Poland 1:50 000, sheet Milowka." Szczegółowa Mapa Geologiczna Polski 1: 50 000, ark. Milówka (1029, M34-87A). Instytut Geologiczny, Warszawa. (in Polish)

[32] Nescieruk, P., and Wójcik, A. 1997. "Detailed Geological Map of Poland 1:50 000, Sheet Bielsko-Biała." Szczegółowa Mapa Geologiczna Polski 1: 50 000, ark. Bielsko Biała (1012, M34-75C). Państwowy Instytut Geologiczny, Warszawa. (in Polish)

[33] Staśko, S., and Tarka, R. 2002. "Supply and drainage of groundwater in mountain areas on the basis of research in the Śnieżnik massif." Zasilanie i drenaż wód podziemnych w obszarach górskich na podstawie badań w masywie Śnieżnika". Acta Univ. Wratisl. Prace Geol.-Mineral., 2528, pp. 1-86. Uniwersytet Wrocławski. Wroclaw. (in Polish)